A&A 496, 645–651 (2009)
DOI: 10.1051/0004-6361/200810709

Astronomy & Astrophysics

The origin of intrinsic variability of intraday variable sources

J. Roland[1], S. Britzen[2], A. Witzel[2], and J. A. Zensus[2]

[1] Institut d'Astrophysique, 98bis Bd Arago, 75014 Paris, France
e-mail: roland@iap.fr
[2] Max-Planck-Institut für Radioastronomie, Auf dem Hügel 69, Bonn 53121, Germany

Received 30 July 2008 / Accepted 4 December 2008

ABSTRACT

Intraday variability (IDV) describes flux-density variations in the radio regime on timescales of a day and less. The origin of such variations has been attributed to both source intrinsic and extrinsic mechanisms. While there is growing evidence that faster flux-density variations (on the order of hours to minutes) are caused by refractive interstellar scattering, extrinsic mechanisms alone still fail to explain all the observations. In particular, in the blazar S5 0716+714, correlated variations at frequencies in the radio and the optical regimes indicate an intrinsic component to the variability. Using the characteristics of the relativistic ejection found for the blazar S5 1803+784, we find that the formation and the rotation of a warp in the inner part of the accretion disk produce a small perturbation of the relativistic beam and consequently a variation in the viewing angle and in the beamed synchrotron emission. We find that the relative flux variations become chaotic if the amplitude of the perturbation exceeds a critical value. We investigate the properties of the chaotic behavior of the solution to explain the observed properties of IDV sources, such as the flux variations, the polarized flux variations, and the observable frequency dependence. As a warp can form naturally in the inner part of the accretion disk, we conclude that both intrinsic and extrinsic mechanisms produce IDV sources.

Key words. radio mechanisms: general – BL Lacertae objects: individual: S5 1803+784 – radio continuum: general

1. Introduction

Intraday variability describes rapid flux-density variations in the radio regime taking place on timescales of one day to a few hours or even minutes (Witzel et al. 1986; Heeschen et al. 1987). For some variable IDV sources, variations have been observed in all frequency regimes: radio, optical, and perhaps even X-rays and γ-ray bands (Wagner & Witzel 1995).

Intraday variations can be produced in the radio band by refractive scintillation in the interstellar medium of our Galaxy (Rickett 1990). Evidence for an extrinsic mechanism comes, e.g., from extreme scattering events observed in the source S5 0954+658 (Fiedler et al. 1987; Cimó et al. 2002) and the so-called annual modulation in S5 0917+624 (Rickett et al. 1995; Fuhrmann et al. 2002). Interstellar scintillation is dominant in very compact objects and at frequencies up to 10 GHz. Any source with a high degree of compactness is bound to scintillate. Scattering has been unequivocally established as a prime mechanism for intraday variability in the case of the source J1819+3845. A 90-s time delay in the arrival times of the source's intensity variations has been measured between two widely-spaced telescopes (Macquart et al. 2003). The tight frequency dependence of the interstellar scattering process predicts that scintillation is suppressed at mm and optical wavelengths.

Thus optical variability alone is caused by an intrinsic mechanism. Possible correlated optical-radio variations observed in compact radio sources stem from intrinsic changes in the sources. Examples of such sources are S5 0716+714 (Quirrenbach et al. 1991) or S5 0954+658 (Wagner et al. 1990).

Compact radio sources show variabilities caused by intrinsic mechanisms. When a new VLBI component is ejected, the optical light curve can show peaks (see, for instance, Britzen et al. 2001 in the case of 0420-014 and Lobanov & Roland 2005 in the case of 3C 345). In that case the optical and radio observations can be understood if the nucleus ejects:

1. a short burst of very energetic $e^{\pm}$ responsible for the optical light curve. This short burst is followed by
2. a long burst of less energetic $e^{\pm}$ responsible for the radio observations of the VLBI component.

These observations indicate that compact radio sources can show variability of intrinsic origin. These variabilities concern the density of the ejected relativistic $e^{\pm}$ and the energy of the ejected relativistic $e^{\pm}$.

In this article, we show that, during the phase with a constant density of ejected $e^{\pm}$, the flux of the unresolved core can vary within a day if the central part of the accretion disk is warped. The rotation of this warp produces a periodic perturbation of the relativistic $e^{\pm}$ beam. The relative flux variations depend on the amplitude R_o of the perturbation and become chaotic if this amplitude becomes greater than a critical value. When the amplitude of the perturbation exceeds this critical value, a small change in the amplitude of the perturbation produces a complete change in the properties of the solution. Although the model is a geometrical model, it is frequency dependent due to opacity effects. We investigate in detail how this model can reproduce the main characteristics of IDV sources, such as the flux variations, the polarized flux variations, and the observable frequency dependence.

In a previous paper (Britzen et al. 2008), we report on 20 years of VLBI observations at 8 and 15 GHz of the source S5 1803+784. Assuming that the nucleus of 1803+784 contains a binary black hole system (BBH system), Roland et al. (2008)

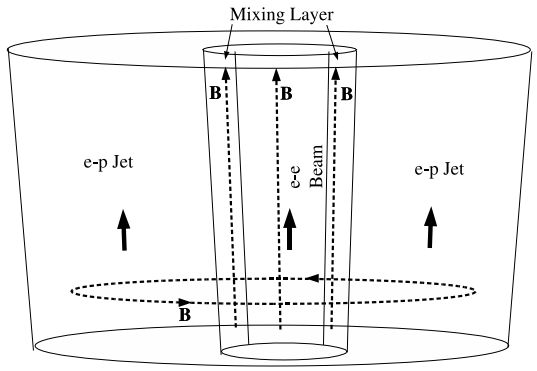

Fig. 1. The two-fluid model. The outflow consists of an $e^- - p$ plasma moving at mildly relativistic speed $v_j \leq 0.4\times c$ and an $e^\pm$ plasma moving at highly relativistic speed (with a corresponding Lorentz factor $\gamma_b \leq 30$). The magnetic field lines are parallel to the flow in the beam and the mixing layer, and are toroidal in the jet.

show how, using the variations $X(t)$ and $Y(t)$ of the VLBI component coordinates, it is possible to determine the inclination angle of the source, the bulk Lorentz factor of the VLBI component, and the characteristics of the families of the BBH systems that provide the same fit of $X(t)$ and $Y(t)$.

Radio flux-density observations of the BL Lac Object S5 1803+784 have been reported by Quirrenbach et al. (1992, 2000) and Kraus et al. (2003). They show slow variability, i.e. day variability (IDV of type I) and fast variability (IDV of type II).

Using the characteristics of the VLBI ejection of 1803+784 (Roland et al. 2008), i.e. the inclination angle, the bulk Lorentz factor, we show that, in the frame of the two-fluid model of radio sources, the properties of the day variability can be explained by the formation and the rotation of a warp in the inner part of the accretion disk.

In Sect. 2, we explain the model and in Sect. 3 we apply the model to the IDV source S5 1803+784.

2. The intraday variability model

2.1. Introduction: the two-fluid model

We describe the ejection of a VLBI component in the frame of the two-fluid model (Sol et al. 1989; Pelletier & Roland 1989, 1990; Pelletier & Sol 1992). The two-fluid description of the outflow is adopted with the following assumptions:

1. the outflow consists of an $e^- - p$ plasma (hereafter *the jet*), moving at mildly relativistic speed $v_j \leq 0.4 \times c$, and an $e^\pm$ plasma (hereafter *the beam*) moving at highly relativistic speed (with corresponding Lorentz factor $\gamma_b \leq 30$);
2. the magnetic field lines are parallel to the flow in the beam and the mixing layer, and are toroidal in the jet (see Fig. 1).

The $e^- - p$ jet carries carries most of the mass and the kinetic energy ejected by the nucleus. It is responsible for the formation of kpc-jets, hot spots, and extended lobes (Muxlow et al. 1988; Roland et al. 1988; Roland & Hetem 1996). The relativistic $e^\pm$ beam moves in a channel through the mildly relativistic jet and is responsible for the formation of superluminal sources and their γ-ray emission (Roland et al. 1994). The relativistic beam can propagate if the magnetic field B is parallel to the flow in the beam and in the mixing layer between the beam and the jet and if it is greater than a critical value (Pelletier et al. 1988; Achatz & Schlickeiser 1993). The magnetic field in the jet becomes rapidly toroidal (Pelletier & Roland 1990). Observational evidence for the two-fluid model has been discussed for example by Roland & Hetem (1996). More recent evidence for the relativistic ejection of an $e^\pm$ beam comes from the γ-ray observations of MeV sources (Roland & Hermsen 1995; Skibo et al. 1997) and from VLBI polarization observations (Attridge et al. 1999). The formation of X-ray and γ-ray spectra, assuming relativistic ejection of $e^\pm$ beams, has been investigated by Marcowith et al. (1995, 1998) in the case of Centaurus A. The possible existence of VLBI components with two different speeds has been recently pointed out in the case of the radio galaxies Centaurus A (Tinglay et al. 1998), Virgo A (Biretta et al. 1999), and 3C 120 (Gomez et al. 2001). If the relativistic beam transfers some energy and/or relativistic particles to the jet, the relativistic particles in the jet will radiate and a new VLBI component with a mildly relativistic speed will be observed. (3C 120 is an example of a source showing this effect.)

2.2. The perturbation model

The synchrotron emission of the so-called core is the emission of the inner part of the relativistic beam, and we suppose that the nucleus ejects a continuous $e^\pm$ plasma. We call *the characteristic length of the unresolved core* the length of the relativistic $e^\pm$ beam that corresponds to the size of the unresolved compact core of the VLBA observations.

The BBH system induces a precession of the accretion disk. The precession period, T_p, is $T_p \propto R_{disk}^{-1.5}$ (Britzen et al. 2001), where R_{disk} is the radius of the accretion disk. Thus, the different parts of the disk will precess with different periods and a warp forms in the disk. The rotation of this warp will produce a perturbation of the magnetic field tube in which the relativistic beam propagates. Let us call V_a the propagation speed of the perturbation[1]. We can determine the flux of the unresolved core by integrating the emission of the beam over the characteristic length of the core.

Let us call Ω the opening angle of the cone on which the beam perturbation will propagate. The coordinates of a point source moving in the perturbed beam are given by

$$x_c = R_o(z)\cos(\omega_p t - k_p z(t) + \phi_o), \quad (1)$$

$$y_c = R_o(z)\sin(\omega_p t - k_p z(t) + \phi_o), \quad (2)$$

$$z_c = z_c(t), \quad (3)$$

where $\omega_p = 2\pi/T_p$, T_p is the rotation period, and k_p is defined by

$$k_p = 2\pi/T_p V_a. \quad (4)$$

We assume that the amplitude of the perturbation first increases linearly and is then damped, we take the form of the amplitude $R(z_c(t))$ to be

$$R(z_c(t)) = \frac{R_o z_c(t)}{(a + z_c(t))}\exp(-t/T_d), \quad (5)$$

where a is

$$a = R_o/(2\ \tan\Omega), \quad (6)$$

and T_d is the characteristic time of the damping of the perturbation.

[1] In this article we use the same notations as in Roland et al. (2008).

The differential equation governing the evolution of $z_c(t)$ can be obtained via the relation for the speed of the component

$$v_c^2 = \left(\frac{dx_c(t)}{dt}\right)^2 + \left(\frac{dy_c(t)}{dt}\right)^2 + \left(\frac{dz_c(t)}{dt}\right)^2, \quad (7)$$

where v_c is related to the bulk Lorentz factor by $v_c/c = \sqrt{(1 - 1/\gamma_c^2)}$.

Using (1)–(3), we find from (7) that dz_c/dt is the solution to the equation

$$A\left(\frac{dz_c}{dt}\right)^2 + B\frac{dz_c}{dt} + C = 0, \quad (8)$$

where the coefficients A, B and C are given by

$$A = 1 + R^2(z_c)k_p^2 \exp(-2t/T_d) + (dR/dz_c)^2 \exp(-2t/T_d), \quad (9)$$

$$B = -2R^2(z_c)\omega_p k_p \exp(-2t/T_d) - 2\frac{dR}{dz_c}\frac{R(z_c)}{T_d}\exp(-2t/T_b), \quad (10)$$

$$C = R^2(z_c)\omega_p^2 \exp(-2t/T_d) + \left(\frac{R(z_c)}{T_d}\right)^2 - v_c^2, \quad (11)$$

which admits two solutions corresponding to the jet and the counter-jet.

We assume that the line of sight is in the plane (yOz) and makes an angle i_o with the z axis. Following Camenzind & Krockenberger (1992), if we call θ the angle between the velocity of the component and the line of sight, we have

$$\cos(\theta(t)) = \left(\frac{dy_c}{dt}\sin i_o + \frac{dz_c}{dt}\cos i_o\right)\Big/ v_c. \quad (12)$$

The Doppler beaming factor δ, characterizing the anisotropic emission of the moving component, is

$$\delta_c(t) = \frac{1}{\gamma_c\,[1 - \beta_c \cos(\theta(t))]}, \quad (13)$$

where $\beta_c = v_c/c$. The observed flux density is

$$S_c = \frac{1}{D^2}\delta_c(t)^{2+\alpha_r}(1+z)^{1-\alpha_r}\int_c j_c dV, \quad (14)$$

where D is the luminosity distance of the source, z its redshift, j_c the emissivity of the component, and α_r the synchrotron spectral index (a negative definition of the spectral index, $S \propto \nu^{-\alpha}$ is used). As the component is moving relativistically toward the observer, the observed time is shortened and given by

$$t_{obs} = \int_0^t [1 - \beta_c \cos(\theta(t'))]\,(1+z)\,dt'. \quad (15)$$

2.3. The flux emission of the core

Let us call Δt the step of the variable t to solve Eq. (8). For each step we determine the coordinate $z_c(t)$ of a point source ejected relativistically in the perturbed beam solving (8). Then, using (1) and (2), we can find the coordinates $x_c(t)$ and $y_c(t)$ of the component. Moreover, for each point we can calculate the derivatives dx_c/dt, dy_c/dt, dz_c/dt and then deduce $\cos\theta$ from (12), δ_c from (13) and consequently S_ν from (14).

Thus the radio flux of the core is

$$S_\nu = \sum_{i=1}^{n} S_\nu(i), \quad (16)$$

where n is the number of points characterizing the length of the beam inside the core.

If we call σ_c the size of the core in milli-arc second units (mas), n is given by

$$n = \sigma_c \times D_a \times \text{mas}/(\sin(i_o)\; c\; \Delta t), \quad (17)$$

where mas is one milli-arc second, i.e. mas $\approx 4.85\times10^{-9}$, and D_a is the angular distance of the source. (It is related to the luminosity distance D_l by $D_a = D_l/(1+z)^2$.)

Although the model is a geometrical model, it is frequency dependent because of opacity effects. Indeed, if we observe at high frequencies, most of the beam of the core will be emitting. The flux of the core at high frequencies is the total flux integrated along the beam. At lower frequencies, due to the synchrotron self-absorption, only the outer part of the beam in the core will be emitting. If we integrate the flux on different fractions of the outer parts of the beam, we model the frequency dependence of the core. In practice, we calculate the flux of the core integrating over 100%, 90%, ... 10% of the outer part of the beam length in the core.

Integrating over 100% of the beam length of the core corresponds to calculating the flux at high frequencies. Integrating over 10% of the outer part of the beam length corresponds to calculating the flux at low frequencies. There is no simple relation between the frequency and integration length along the beam. However, integrating over 10% will correspond to frequencies around 5 GHz, and integrating over 100% will correspond to optical synchrotron radiation.

2.4. The linearly and circularly polarized emission of the core

As indicated in Pelletier & Roland (1990), the mildly relativistic jet produces a Faraday rotation and a depolarization of the synchrotron emission of the relativistic beam. Close to the nucleus, the magnetic field in the jet is not toroidal and will produce a strong Faraday rotation. No linear polarization will be observed. When the jet advances, the magnetic field becomes toroidal and the linear polarization of the synchrotron emission of the beam can be observed, so the linearly polarized emission of the core will be the emission of a fraction of the length of the core. The fraction of the beam emitting the linearly polarized emission will be the outer part of the beam inside the core.

The linear polarized flux of the core is then

$$S_{\text{lin-pol}} = \sum_{i=n-n_{lp}}^{n} S_{\text{lin-pol}}(i), \quad (18)$$

where n and n_{lp} are respectively the number of points characterizing the length of the beam and the length of the linear polarized part of the beam in the core. Calling the size of the unresolved

core σ_c, we will choose for the size of the linear polarized part of the beam in the core $\sigma_{c,lin-pol} \approx \sigma_c/3$.

A variation in the viewing angle will produce a variation in the beamed polarized emission. As the integration length of the polarized emission is less than the integration length of the unpolarized emission, the changes in the fluxes of the polarized and the unpolarized emission will be different. Moreover, during this change due to a very small change in the viewing angle, the position angle of the polarized emission will not change.

In addition to linear polarization variations, compact radio sources can show strong relative circular polarization variations (Macquart et al. 2000; Homan & Lister 2006). The circular polarization occurs in the outer part of the linearly polarized beam. We choose for the size of the circularly polarized part of the beam $\sigma_{c,cir-pol} \approx \sigma_c/10$.

3. Application to 1803+784

The blazar S5 1803+784 ($z \approx 0.68$, Lawrence et al. 1987; Stickel et al. 1993) is an intraday variable source with rapid flux-density variations in the optical and radio regime (Wagner & Witzel 1995; Quirrenbach et al. 1992, 2000; Kraus et al. 2003) on timescales as short as 50 min in the optical (Wagner et al. 1990). It has been observed and studied with different VLBI arrays at a range of different frequencies (e.g., Eckart et al. 1986, 1987; Witzel et al. 1988; Charlot 1990; Strom & Biermann 1991; Fey et al. 1996; Gabuzda 1999; Gabuzda & Cawthorne 2000; Gabuzda & Chernetskii 2003; Ros et al. 2000, 2001; Britzen et al. 2005a,b, 2008).

An analysis of almost 20 years of VLBI observations at 8 and 15 GHz has been performed by Britzen et al. (2008). Assuming that the nucleus of 1807+784 contains a BBH system, from the knowledge of the variations of the VLBI component coordinates, Roland et al. (2008) determine the inclination of the source to be $i_o \approx 5.8^{\circ\,+1.7}_{-1.8}$. The VLBI component is ejected with a bulk Lorentz factor of $\gamma \approx 3.7^{+0.3}_{-0.2}$.

3.1. The short-term variations: modeling

If a warp forms in the inner part of the accretion disk, it will rotate and will perturb the magnetic tube in which the $e^{\pm}$ plasma is ejected. The perturbation will propagate with speed V_a and will move on a cone of opening angle Ω. As the perturbation is due to a warp in the inner part of the accretion disk, it concerns only the central part of the $e^- - p$ jet, and it will produce a very small perturbation of the $e^{\pm}$ beam. Consequently, the angle Ω will be very small, and we choose $\Omega_o \approx 0.01^{\circ}$. The amplitude of the perturbation is described by the parameter R_o (see Eq. (5)). This parameter R_o is a free parameter, and we calculate the relative flux variations as a function of R_o.

The flux of a point source is $S_\nu \propto \delta_c^{2+\alpha_r}$, see Eq. (14). Thus, close to the nucleus we model the shape of the flux of a point component at $z_c = z_c(t)$ by

$$S_\nu(z_c) = \delta_c^{2+\alpha_r} \exp(-T_{ro}/t) \times \exp(-t/T_{r1})/S_{scale}, \quad (19)$$

where T_{ro}, T_{r1}, and S_{scale} are respectively a characteristic timescale to describe the radio opacity, a characteristic timescale to describe the radiative losses, and a scaling factor[2]. The total flux of the core is then given by Eq. (16).

We modeled the short-term variation in the following way. At a given time t_o, assuming a continuous ejection of the $e^{\pm}$ beam, we calculated the flux of the unresolved core using Eq. (16). For the time $t_o + \Delta t$, we calculated the new flux of the core changing the phase ϕ_o in Eqs. (1) and (2). As the flux is known with an arbitrary constant, we normalized the flux dividing the calculated flux at t by $S_\nu(t_o)$. This has the advantage to determine the relative flux variations and not the absolute flux at a given moment. The values used for T_{ro}, T_{r1} and S_{scale} in Eq. (19) are not important here. We arbitrarily chose $T_{ro} = 5$ yrs, $T_{r1} = 50$ yrs, and $S_{scale} = 0.01$.

Using the results of Roland et al. (2008), the values of the parameters are:

- $i_o \approx 5.8^{\circ}$ for the inclination;
- $z \approx 0.68$ for the redshift;
- $V_a \approx 0.0484 \times c$ for the propagation speed of the perturbations[3];
- $\sigma_c \approx 0.1$ mas for the size of the unresolved core;
- $\sigma_{c,lin-pol} \approx \sigma_c/3$ for the size of the linearly polarized part of the beam in the core (see Sect. 2.4);
- $\sigma_{c,cir-pol} \approx \sigma_c/10$ for the size of the circularly polarized part of the beam in the core (see Sect. 2.4);
- $\gamma_c \approx 3.7$ for the bulk Lorentz factor of the ejected $e^{\pm}$ plasma;
- $\Omega_o \approx 0.01^{\circ}$ for the opening angle of the cone;
- $T_p \approx 4$ days for the perturbation period;
- $T_d \approx 100$ yr for the timescale of the damping of the beam perturbations;
- R_o is a free parameter.

We wish to point out that we do not try to make a fit of the observations, but we here present a qualitative way to explain the observations by a geometrical model that is intrinsic to the source. The set of parameters we discuss here is not unique.

3.2. The short-term variations: results

We calculated the relative flux variations of the core when the parameter R_o changes. As indicated previously, the perturbation is weak and the parameter R_o will be small. The result of the calculation is shown in Fig. 2.

The main result is the existence of a critical value, $R_{o,c} \approx 10^{-6}$ pc:

- if $R_o \leq 10^{-6}$ pc, the relative flux variations change regularly when the parameter R_o changes;
- if $R_o > 10^{-6}$ pc, the relative flux variations become chaotic; i.e. their amplitude changes very rapidly when R_o changes. For instance, $\Delta S/S \approx 8\%$ if $R_o \approx 1.2625 \times 10^{-5}$ pc but $\Delta S/S \approx 80\%$ if $R_o \approx 1.3125 \times 10^{-5}$ pc (see Fig. 3).

This chaotic behavior of the solution has fundamental consequences for the observed relative flux variations.

The first consequence concerns the nonperiodic variability of the flux variations. If there is a warp in the central part of the accretion disk and if the rotation period of the warp is constant, a small change of the amplitude of the perturbation will produce large changes of the observed relative flux variations producing an apparently nonperiodic and extremely variable source.

The second consequence concerns the apparent timescale of the observed flux variations. We plotted in Fig. 3 the flux variations corresponding to $R_o \approx 1.3125 \times 10^{-5}$ pc

[2] If the component is close to the core, the shape of the flux can be described by (19) if $T_{ro} \ll T_{r1}$

[3] This value corresponds to the solution S1c of the family S1 (see Appendix B in Roland et al. 2008).

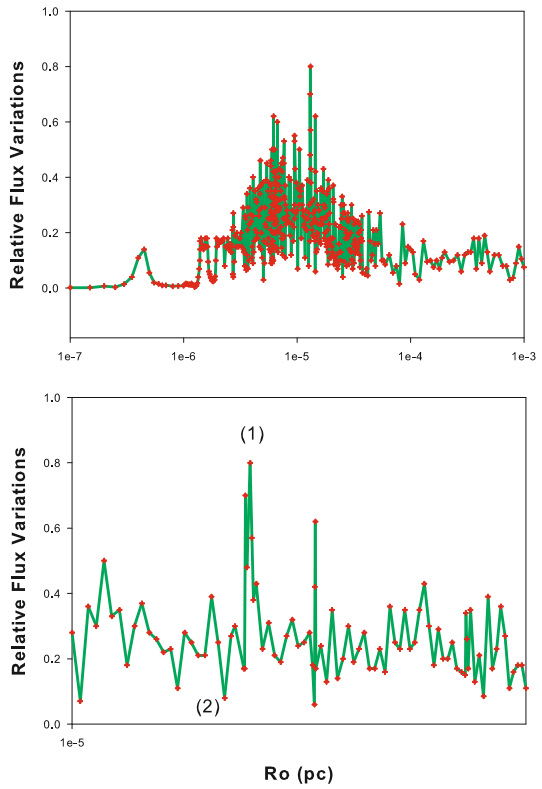

Fig. 2. Relative flux variations as a function of R_o. The relative flux variation is defined as the ratio $S_\nu(t)/S_\nu(t_o)$ (see Sect. 3.1). They have been calculated integrating over the total length of the beam in the core for 10^{-7} pc $\leq R_o \leq 10^{-3}$ pc (see Sect. 2.3). *Top figure*: the flux variations are regular when $R_o \leq 10^{-6}$ pc and become chaotic when $R_o > 10^{-6}$ pc. *Bottom figure*: relative flux variations as a function of R_o for 10^{-5} pc $\leq R_o \leq 2 \times 10^{-5}$ pc. In this article we study the two cases corresponding to $R_o \approx 1.3125 \times 10^{-5}$ pc and $R_o \approx 1.2625 \times 10^{-5}$ pc, which are labeled respectively as (1) and (2).

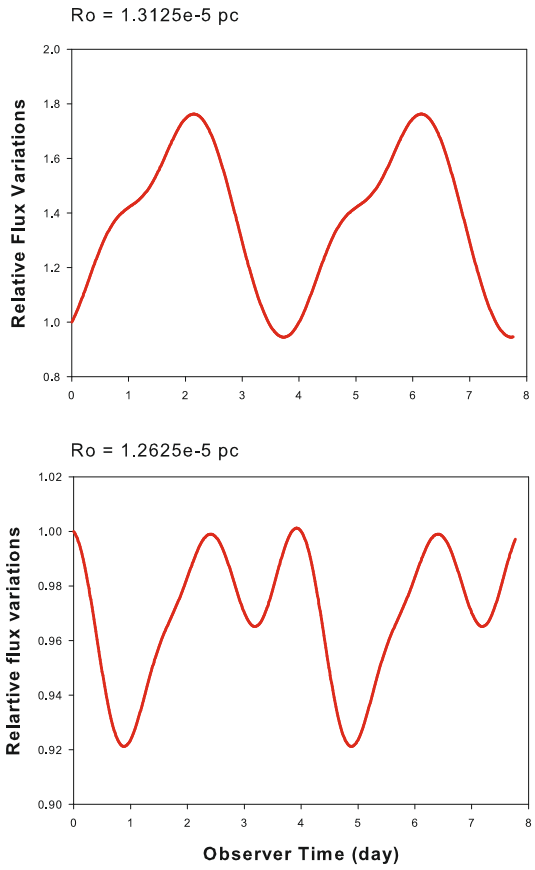

Fig. 3. Relative flux variations as a function of time. They have been calculated by integrating over the total length of the beam in the core. *Top figure*: in the case $R_o \approx 1.3125 \times 10^{-5}$ pc, the total flux changes of ≈80% with a typical timescale of about 2 days. *Bottom figure*: in the case $R_o \approx 1.2625 \times 10^{-5}$ pc, the total flux changes of 4% to 8% with a typical timescale of about 1 day.

and $R_o \approx 1.2625 \times 10^{-5}$ pc. We see that the typical timescale of the observed flux variations is 2 days in the case corresponding to $R_o \approx 1.3125 \times 10^{-5}$ pc, but the typical timescale of the observed flux variations is 1 day in the case corresponding to $R_o \approx 1.2625 \times 10^{-5}$ pc.

The third consequence concerns the frequency behavior of the flux variations. As indicated previously, although the model is a geometrical model, it is frequency dependent due to opacity effects (see Sect. 2.3). The results corresponding to $R_o \approx 1.3125 \times 10^{-5}$ pc and to $R_o \approx 1.2625 \times 10^{-5}$ pc are shown in Figs. 4 and 5, respectively.

In the case corresponding to $R_o \approx 1.3125 \times 10^{-5}$ pc, the flux variations are mostly independent of the fraction of the outer part of the beam if this fraction is greater or equal to 50%. However, if this fraction is less than 50%, the flux variation is weakly dependent on this fraction, but changes a lot if the fraction is about 30%. As a result, in the case $R_o \approx 1.3125 \times 10^{-5}$ pc, the flux variations:

- will mostly be independent on the frequency at high frequencies;
- will weakly be dependent on the frequency at low frequencies; and
- will present a large variation ($\Delta S/S \approx 120\%$) around a given frequency.

However, in the case corresponding to $R_o \approx 1.2625 \times 10^{-5}$ pc, even at high frequencies, the flux variations depend strongly on the fraction of the outer part of the beam to calculate the flux. For instance, the relative flux variations of the core is $(\Delta S/S)_{0.1\ \mathrm{mas}} \approx 8\%$, but the flux variations of the half outer part of the beam is $(\Delta S/S)_{0.05\ \mathrm{mas}} \approx 18\%$. Moreover, at low frequencies, the flux variations increase when the frequency decreases.

In the case $R_o \approx 1.2625 \times 10^{-5}$ pc, the flux variations:

- will be dependent on the frequency at high and low frequencies;
- at low frequencies, will increase when the frequency decreases; and
- can be $\Delta S/S \approx 130\%$ at the lowest frequency.

The fourth consequence of the model concerns the day variability of the linearly polarized flux of the core. As indicated in Sect. 2.4, the polarized flux comes from the outer part of the beam in the core. With $\sigma_{c,\mathrm{lin:pol}} \approx \sigma_c/3$, we calculated the polarized flux variations. The variations corresponding to $R_o \approx 1.2625 \times 10^{-5}$ pc are shown in Fig. 6. The relative polarized flux variations are greater than the relative flux variation, i.e. $(\Delta S/S)_{\mathrm{lin:pol}} \approx 35\%$ and $\Delta S/S \approx 8\%$. This is generally the case if $\sigma_{c,\mathrm{lin:pol}} \approx \sigma_c/3$ and $R_o > R_c \approx 10^{-6}$ pc. However, if the value of $\sigma_{c,\mathrm{lin:pol}}$ changes, the relative polarized flux variations can be less than the relative flux variations.

The fifth consequence of the model concerns the day variability of the circularly polarized flux variations of the core. Compact radio sources can show strong relative circular polarization variations. The circular polarization arises in the outer

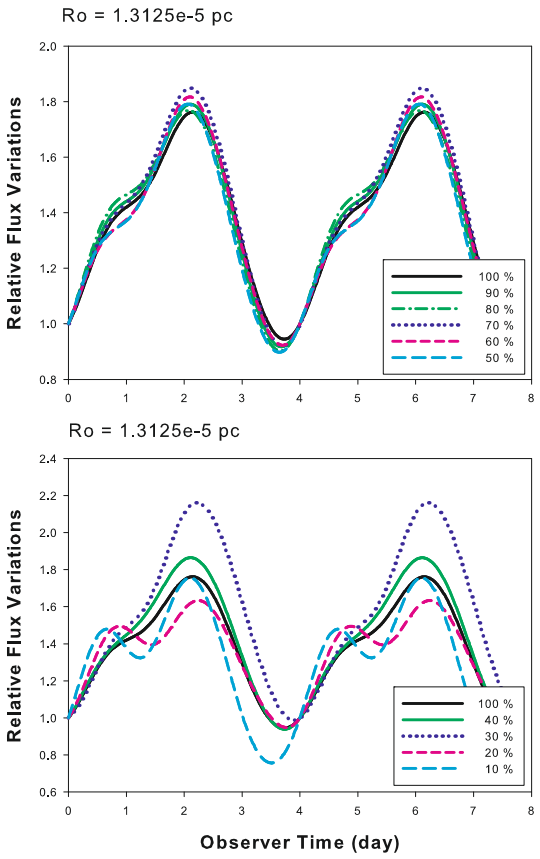

Fig. 4. Relative flux variations as a function of time for $R_o \approx 1.3125 \times 10^{-5}$ pc. *Top*: they have been calculated for different fractions of the outer part of the beam in the core (100%, 90% ... 50%). At high frequencies, the flux variations are mostly independent of the observing frequency. *Bottom*: they have been calculated for different fractions of the outer part of the beam in the core (100%, 40% ... 10%). At low frequencies, the flux variations depend weakly on the frequency, except around a given frequency corresponding to an integration length of 30% of the outer part of the beam.

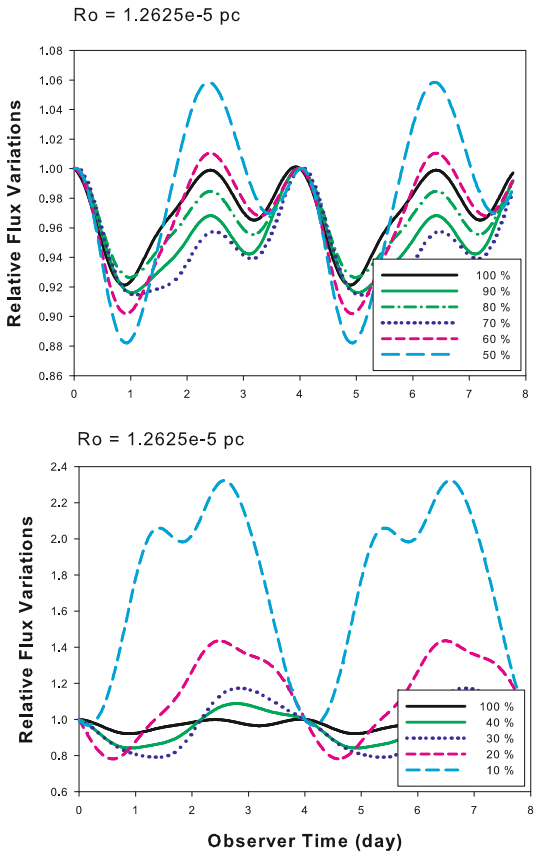

Fig. 5. Relative flux variations as a function of time for $R_o \approx 1.2625 \times 10^{-5}$ pc. *Top*: they have been calculated for different fractions of the outer part of the beam in the core (100%, 90% ... 50%). At high frequencies, the flux variations depend on the observing frequency. *Bottom*: they were calculated for different fractions of the outer part of the beam in the core (100%, 40% ... 10%). At low frequencies, the flux variations increase when the frequency decreases.

part of the linearly polarized beam; i.e. as indicated in Sect. 2.4, we assume that $\sigma_{c,cir:pol} \approx \sigma_c/10$.

If $R_o \approx 1.3125 \times 10^{-5}$ pc, we find that $(\Delta S/S)_{cir:pol} \leq (\Delta S/S)_{lin:pol}$ (see Fig. 4). However, if $R_o \approx 1.2625 \times 10^{-5}$ pc, we see from Fig. 5 than $(\Delta S/S)_{cir:pol} \approx 130\%$ and $(\Delta S/S)_{lin:pol} \approx 40\%$.

4. Discussion and conclusion

If compact radio sources show some variabilities that can be explained by an extrinsic mechanism, they show any variabilities due to intrinsic mechanisms.

When a new VLBI component is ejected, the optical light curve can show peaks (see for instance, Britzen et al. 2001 in the case of 0420-014; and Lobanov & Roland 2005 in the case of 3C 345). In that case the optical and radio observations can be understood if the nucleus ejects:

1. a short burst of very energetic $e^{\pm}$ responsible for the optical light curve. This short burst is followed by

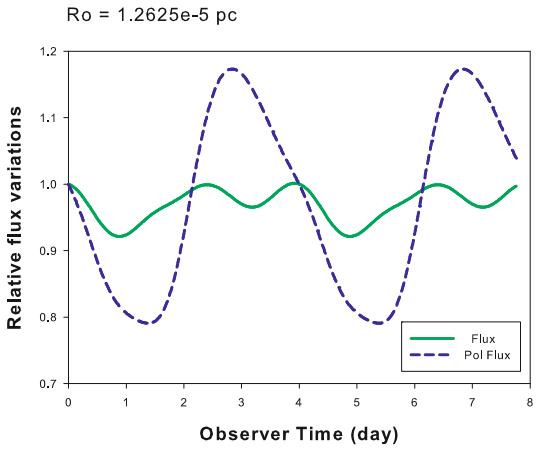

Fig. 6. Relative flux variations and relative linear polarized flux variation corresponding to $R_o \approx 1.2625 \times 10^{-5}$ pc assuming $\sigma_{c,lin:pol} \approx \sigma_c/3$. The relative polarized flux variations are larger than the relative flux variations.

2. a long burst of less energetic $e^{\pm}$ responsible for the radio observations of the VLBI component[4].

[4] In the case of 1803+784, Roland et al. (2008) found that the duration of the ejection of the $e^{\pm}$ plasma responsible for the VLBI component is ≈14.5 yr in the BBH system frame.

These observations indicate that compact radio sources can show intrinsic variabilities. These variabilities concern

1. the density of the ejected $e^{\pm}$;
2. the energy of the ejected relativistic $e^{\pm}$.

In this article, we show that, during the phase with a constant density of ejected $e^{\pm}$, the flux of the unresolved core can vary within a day if the central part of the accretion disk is warped. The rotation of this warp produces a periodic perturbation of the relativistic $e^{\pm}$ beam. The relative flux variations depend on the amplitude R_o of the perturbation and become chaotic if this amplitude becomes greater than a critical value. When the amplitude of the perturbation is greater than the critical value, a small change in the amplitude of the perturbation produces a complete change in the properties of the solution. The main properties of the solution can be summarized as follows. A periodic perturbation of the relativistic beam can produce:

1. An apparently non periodic and extremely variable source.
2. Flux variations, where the timescale varies by a factor 2.
3. Flux variations, where the frequency dependence can change with time following at least 2 different regimes, i.e. either the flux variations:
   - will be mostly independent on the frequency at high frequencies;
   - will be weakly dependent on the frequency at low frequencies; and
   - will present a large variation ($\Delta S/S \approx 120\%$) around a given frequency.

   Or they
   - will be dependent on the frequency at high and low frequencies;
   - at low frequencies, will increase when the frequency decreases;
   - can be $\Delta S/S \approx 130\%$ at the lowest frequency.
4. Relative linearly polarized flux variations generally larger than the relative flux variations.
5. Relative circularly polarized flux variations either larger or smaller than the relative linear polarized flux variations.

The properties of the model correspond to the observational properties of IDV sources.

During the phase of ejection of the relativistic $e^{\pm}$ with a constant density, the formation and the rotation of a warp in the inner part of the accretion disk produce a day variability of the compact core. This effect happens naturally, and as the fastest variations can be explained by refractive interstellar scattering, *we conclude that both intrinsic and extrinsic mechanisms occur producing the observed variability of compact radio sources.*

References

Achatz, U., & Schlickeiser, R. 1993, A&A, 274, 165
Attridge, J. M., Roberts, D. H., & Wardle, J. F. C. 1999, ApJ, 518, 87
Benford, G., & Lesch, H. 1998, MNRAS, 301, 414
Biretta, J. A., Sparks, W. B., & Macchetto, F. 1999, ApJ, 520, 621
Britzen, S., Roland, J., Laskar, J., et al. 2001, A&A, 374, 784
Britzen, S., Krichbaum, T. P., Strom, R. G., et al. 2005a, A&A, 444, 443
Britzen, S., Witzel, A., Krichbaum, T. P., et al. 2005b, MNRAS, 362, 966
Britzen, S., Kudryavtseva, N. A., Beckert, T., et al. 2008, in prep.
Camenzind, M., & Krockenberger, M. 1992, A&A, 255, 59
Charlot, P. 1990, A&A, 229, 51
Cimó, G., Beckert, T., Krichbaum, T. P., et al. 2002, PASA, 19, 10
Eckart, A., Witzel, A., Biermann, P., et al. 1986, A&A, 168, 17
Eckart, A., Witzel, A., & Biermann, P. 1987, A&AS, 67, 121
Fey, A. L., Clegg, A. W., & Fomalont, E. B. 1996, ApJS, 105, 299
Fiedler, R. L., Dennison, B., Johnston, K. J., et al. 1987, Nature, 326, 675
Fuhrmann, L., Krichbaum, T. P., Cimó, G., et al. 2002, PASA, 19, 64
Gabuzda, D. C. 1999, NewAR, 43, 691
Gabuzda, D. C., & Cawthorne, T. V. 2000, MNRAS, 319, 1056
Gabuzda, D. C., & Chernetskii, V. A. 2003, MNRAS, 339, 669
Gomez, J.-L., Marscher, A. P., Alberdi, A., Jorstad, S. G., & Agudo, I. 2001, ApJ, 521, L161
Heeschen, D. S., Krichbaum, T., Schalinski, C. J., & Witzel, A. 1987, AJ, 94, 1493
Homan, D. C., & Lister, M. L. 2006, AJ, 131, 1262
Kraus, A., Krichbaum, T. P., Wegner, R., et al. 2003, A&A, 401, 161
Lawrence, C. R., Readhead, A. C. S., Pearson, T. J., & Unwin, S. C. 1987, in Superluminal Radio Sources, ed. J. A. Zensus, & T. J. Pearson (Cambridge: Cambridge University Press), 260
Lobanov, A., & Roland, J. 2005, A&A, 431, 831
Macquart, J.-P., Kedziora-Chudczer, L., Rayner, D. P., & Jauncey, D. L. 2000, ApJ, 538, 623
Macquart, J. P., de Bryun, A. G., & Dennett-Thorpe, J. 2003, ASPC, 290, 349
Marcowith, A., Henri, G., & Pelletier, G. 1995, MNRAS, 277, 681
Marcowith, A., Henri, G., & Renaud, N. 1998, A&A, 331, L57
Muxlow, T. W. B., Pelletier, G., & Roland, J. 1988, A&A, 206, 237
Nesci, R., Massaro, E., Rossi, C., et al. 2005, AJ, 130, 1466
Pelletier, G., & Roland, J. 1989, A&A, 224, 24
Pelletier, G., & Roland, J. 1990, in Parsec-Scale Jets, ed. J. A. Zensus, & T. J. Pearson (Cambridge: Cambridge University Press), 323
Pelletier, G., & Sol, H. 1992, MNRAS, 254, 635
Pelletier, G., Sol, H., & Asseo, E. 1988, Phys. Rev. A, 38, 2552
Qian, S. J., Quirrenbach, A., Witzel, A., et al. 1991, A&A, 241, 15
Quirrenbach, A., Witzel, A., Wagner, S., et al. 1991, ApJ, 372, L71
Quirrenbach, A., Witzel, A., Krichbaum, T. P., et al. 1992, A&A, 258, 279
Quirrenbach, A., Kraus, A., Witzel, A., et al. 2000, A&AS, 141, 221
Rickett, B. J. 1990, ARA&A, 28, 561
Rickett, B. J., Quirrenbach, A., Wegner, R., Krichbaum, T. P., & Witzel, A. 1995, A&A, 293, 479
Roland, J., & Hermsen, W. 1995, A&A, 297, L9
Roland, J., & Hetem, A. 1996, in Cygnus A: Study of a radio galaxy, ed. C. L. Carilli, & D. E. Harris (Cambridge: Cambridge University Press), 126
Roland, J., Peletier, G., & Muxlow, T. 1988, A&A, 207, 16
Roland, J., Teyssier, R., & Roos, N. 1994, A&A, 290, 357
Roland, J., Britzen, S., Kudryavtseva, N. A., Witzel, A., & Karousos, M. 2008, A&A, 483, 125
Ros, E., Marcaide, J. M., Guirado, J. C., et al. 2000, A&A, 356, 357
Skibo, J. G., Dermer, C. D., & Schlickeiser, R. 1997, ApJ, 483, 56
Sol, H., Pelletier, G., & Asseo, E. 1989, MNRAS, 237, 411
Stickel, M., Fried, J. W., & Kühr, H. 1993, A&AS, 98, 393
Strom, R. G., & Biermann, F. L. 1991, A&A, 242, 313
Tingay, S. J., Jauncey, D. L., Reynolds, J. E., et al. 1998, AJ, 115, 960
Wagner, S., Sanchez-Pons, F., Quirrenbach, A., & Witzel, A. 1990, A&A, 235, L1
Wagner, S. J., & Witzel, A. 1995, ARA&A, 33, 163
Witzel, A., Heeschen, D. S., Schalinski, C., & Krichbaum, Th. 1986, Mitteilungen der Astronomischen Gesellschaft, 65, 239
Witzel, A., Schalinski, C. J., Johnston, K. J., et al. 1988, A&A, 206, 245